An inverted continental Moho and serpentinization of the forearc mantle

M. G. Bostock*, R. D. Hyndman†‡, S. Rondenay*§ & S. M. Peacock‖

** Department of Earth and Ocean Sciences, The University of British Columbia, Vancouver, British Columbia V6T 1Z4, Canada*
† Pacific Geoscience Centre, Geological Survey of Canada, Sidney, British Columbia V8L 4B2, Canada
‡ School of Earth and Ocean Sciences, University of Victoria, British Columbia V8W 3P6, Canada
‖ Department of Geological Sciences, Arizona State University, Tempe, Arizona 85287-1404, USA

Volatiles that are transported by subducting lithospheric plates to depths greater than 100 km are thought to induce partial melting in the overlying mantle wedge, resulting in arc magmatism and the addition of significant quantities of material to the overlying lithosphere[1]. Asthenospheric flow and upwelling within the wedge produce increased lithospheric temperatures in this back-arc region, but the forearc mantle (in the corner of the wedge) is thought to be significantly cooler. Here we explore the structure of the mantle wedge in the southern Cascadia subduction zone using scattered teleseismic waves recorded on a dense portable array of broadband seismometers. We find very low shear-wave velocities in the cold forearc mantle indicated by the exceptional occurrence of an 'inverted' continental Moho, which reverts to normal polarity seaward of the Cascade arc. This observation provides compelling evidence for a highly hydrated and serpentinized forearc region[2], consistent with thermal and petrological models of the forearc mantle wedge. This serpentinized material is thought to have low strength and may therefore control the down-dip rupture limit of great thrust earthquakes, as well as the nature of large-scale flow in the mantle wedge.

In 1993–94, researchers at the Oregon State University deployed about 40 seismometers at 69 sites across central Oregon as part of an IRIS-PASSCAL experiment to investigate detailed structure of the Cascadia subduction zone[3] (Fig. 1). Stations were located at intervals of 5 km, and recorded high-quality P-wave seismograms from 31 earthquakes at teleseismic (30–100°) distances. The array geometry and station density permit the application of formal, multichannel waveform inversions of scattered waves arriving after the direct P-wave that are generated by discontinuous structure below the array[4,5]. These scattered waves include both forward-scattered P-wave-to-S-wave conversions and back-scattered waves afforded by free-surface reflections, and are sensitive to discontinuities in shear-wave velocity and density.

In Fig. 2a we display an image of S-wave velocity perturbations beneath central Oregon as determined from the simultaneous inversion of scattered waves from the 31 earthquakes. The perturbations are defined with respect to a smoothly varying, one-dimensional reference model. The limited frequency content of the scattered wave data results in a bandpass-filtered approximation to the true perturbation structure. Planar discontinuities are therefore defined by rapid transitions from high/low to low/high velocity perturbations. Two prominent structures dominate the image in Fig. 2a. The continental Moho is evident as a boundary near 36 km depth across the eastern portions (east of −122.3° longitude) of the section, where it separates low-velocity (shown red) continental crust from high-velocity (shown blue) mantle. The Moho persists seaward to approximately 40 km west of the arc, beyond which it apparently disappears. At the western edge of the profile we note an approximately 10-km-thick, low-velocity layer centred at 25 km depth, which dips shallowly at ~10°. As in an earlier forward modelling study employing the same data set[3], this layer is associated with the oceanic crust of the subducting Juan de Fuca plate. By 45 km depth, the oceanic Moho (lower boundary of oceanic crust) dips more steeply (~30°) and exhibits a reduced velocity contrast. It can be traced to a depth of ~90 km towards the eastern end of the profile. The upper boundary of subducted Juan de Fuca crust appears to possess a landward evolution that is more complex than that of the underlying Moho. At 30 km depth, the upper-crustal boundary apparently levels off and adopts a horizontal trajectory with diminishing velocity contrast to the east. The relation of this subhorizontal boundary with the continental Moho further landward, or with the dipping oceanic Moho below, is unclear. However, there is an absence of strongly discontinuous structure in the intervening volume.

To understand the nature of these variations in velocity structure, we need to consider the water budget of the downgoing oceanic crust, the effects of hydration on mantle peridotite, and temperatures across the subduction complex. It is generally understood that significant quantities of aqueous fluid are expelled from the downgoing crust and sediments as they encounter increasing pressure and temperature[6]. Much of this fluid is driven off at shallow levels, but estimates of fluid fluxes based on core and downhole measurements[7] suggest that, over 10–20 Myr, sufficient H_2O is released at subcrustal levels to hydrate the entire forearc mantle. Hydration of depleted peridotite (the dominant mantle rock type comprising olivine, orthopyroxene and lesser amounts of clinopyroxene and Cr-spinel) will stabilize a variety of hydrous minerals, in particular, serpentine[8]. The stable mineral assemblage will depend on temperature, pressure and bulk composition, especially SiO_2 content. In addition to serpentine minerals, hydrated peridotite may contain additional hydrous minerals, such as amphibole, brucite, chlorite and talc. Antigorite is the main serpentine mineral in ultramafic rocks metamorphosed under moderate temperatures, and is stable to temperatures of 620–720 °C at depths between 30 and 150 km (ref. 9).

In addition to supplying the fluids that hydrate the overlying

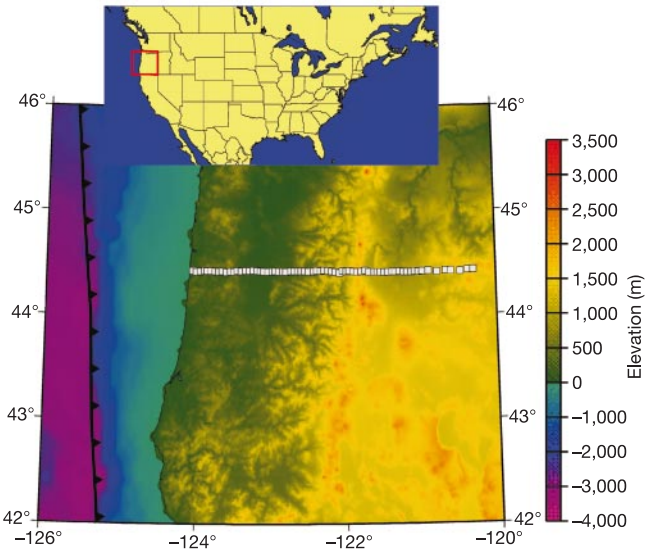

Figure 1 Relief map of central Cascadia subduction zone. Locations of broadband, three-component seismic stations that recorded the data employed in this study are shown as white squares. Note that the array is oriented approximately perpendicular to the strike of major topographic features associated with the subduction zone.

§ Present address: Department of Geological Sciences, Brown University, Providence, Rhode Island 02912, USA

mantle wedge, the subducting plate also controls the thermal structure of the subduction-zone forearc. In particular, it significantly depresses isotherms in the mantle wedge, as evidenced by the very low surface heat flow (30–40 mW m^{-2}) observed in most forearcs including Cascadia[10,11]. In Fig. 2b we plot a thermal model for central Oregon[12] corresponding to the teleseismic profile, and based on heat flow and other geophysical data. In the region where oceanic crust meets the forearc mantle, temperatures are low, between 400 and 600 °C, a situation that persists over a horizontal distance of ~50–100 km. However, a landward increase in heat flow from <40 to >80 mW m^{-2} over ~20 km signals an abrupt increase in deep temperatures. In particular, Moho temperatures beneath the arc and backarc are significantly higher, above 800 °C. Thus serpentine should exist in that portion of the mantle forearc contained within the dashed square in Fig. 2b, but it will not be stable beneath the arc and backarc. The degree of serpentinization in the forearc will depend upon the amount of H_2O that chemically interacts with forearc mantle, which, in turn, depends on H_2O flux from the subducting slab and the permeability structure of the slab, plate interface and mantle.

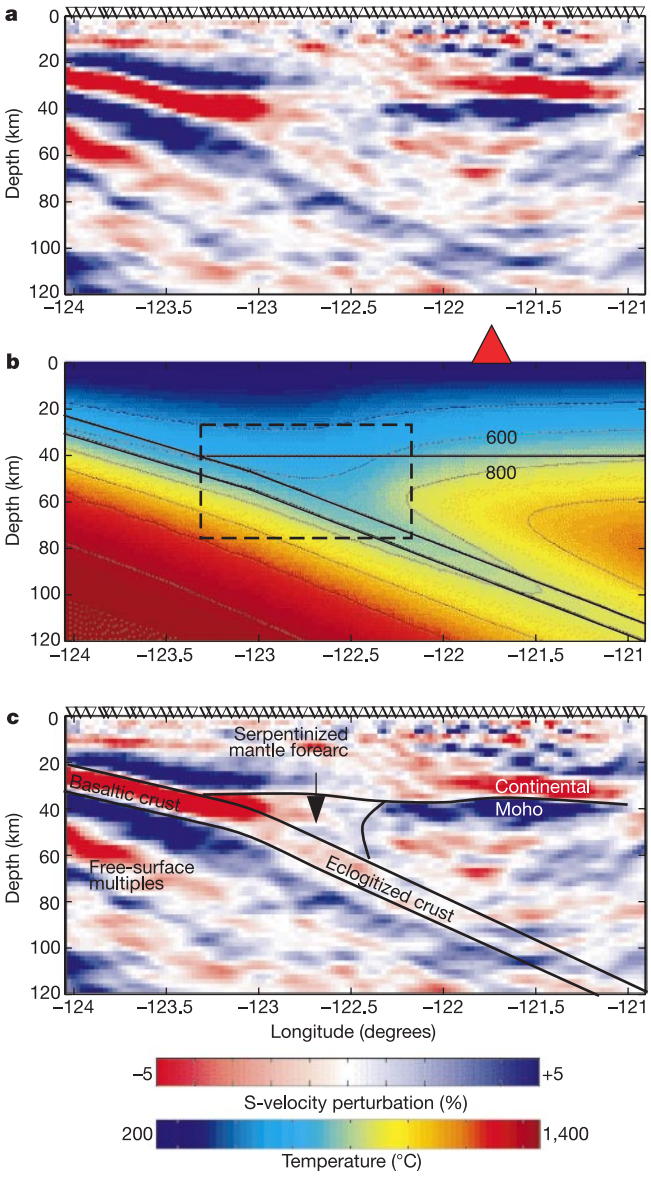

Figure 2 Comparison of scattered wave inversion results with thermal model. **a**, S-velocity perturbations below the array, recovered from the inversion of scattered waves in the P-wave coda of 31 earthquakes recorded at teleseismic distances. The image represents a bandpass-filtered version of the true perturbations to a one-dimensional, smoothly varying reference model. Discontinuities are present where steep changes in perturbation polarity occur. **b**, Thermal model of Cascadia subduction zone corresponding approximately to the profile in **a**. The cool subducting plate depresses isotherms in the forearc, rendering serpentine stable within that portion of the mantle encompassed by the dashed rectangle; solid lines indicate locations of subducting oceanic crust and continental Moho. Note temperature contour interval is 200 °C. **c**, Interpretation of structure in **a**. High degrees of mantle serpentinization where the subducting oceanic crust enters the forearc mantle results in an inverted continental Moho (high-velocity crust on low-velocity mantle), which gradually reverts eastward to normal polarity by −122.3° longitude. The signature of the subducting oceanic Moho diminishes with depth as a result of progressive eclogitization below 45 km. Inverted triangles in **a** and **c** show instrument locations.

Serpentinite exhibits elastic properties that are unique among commonly occurring rock types, notably low elastic wave velocities and high Poisson's ratio. The very low S-velocity of serpentinite is central to the interpretation of our results. In particular, its S-velocity (v_S) is significantly lower than that of its peridotitic protolith ($\delta v_S \approx -2$ km s^{-1}) and commonly occurring lower-crustal lithologies ($\delta v_S \approx 1$ km s^{-1})[13]. Figure 3 shows the S-wave velocity of mantle peridotite samples as a function of degree of serpentinization at a pressure of 1 GPa, which is appropriate for the base of a ~35-km-thick continental crust as presented in ref. 14. Correction from room temperature to 400–500 °C will shift this curve downward to velocities 0.1–0.2 km s^{-1} lower. This information allows us to interpret the image in Fig. 2a quantitatively in terms of degree of serpentinization in the forearc mantle. As in a previous study[3], we interpret the change in dip of the subducting plate by 45 km depth to indicate the onset of eclogitization of the oceanic crust, leading, eventually, to a 15% increase in density and a pronounced reduction in the seismic contrast with underlying oceanic mantle[15].

Although a continuous dehydration of downgoing oceanic crust and entrained sediments is expected, the water released by eclogitization (between 1.2 and 3.3 wt%; ref. 16) is especially important for expulsion into the overlying mantle wedge, where it causes hydration and serpentinization, and significantly diminished velocities. The horizontal boundary near 32 km depth and between −122.6 and −123.3° longitude that juxtaposes high- (or neutral-) velocity material above with low-velocity material below is thus inferred to manifest the highly unusual occurrence of an 'inverted' continental Moho separating lower-crustal rocks from underlying,

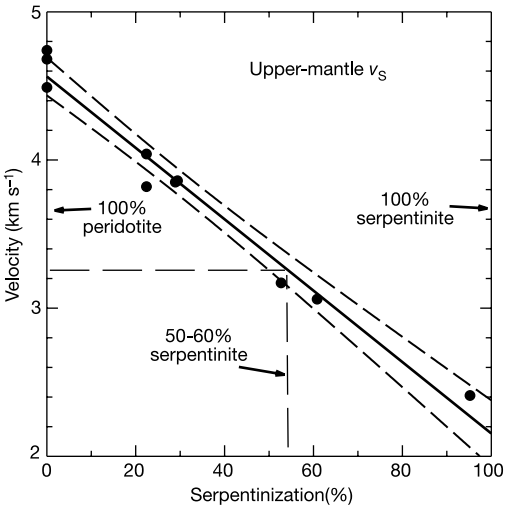

Figure 3 S-velocity of altered peridotite as a function of degree of serpentinization. Data from ref. 14. Bold line shows best-fit linear regression with ±1σ error bounds. The predicted velocity contrast at the wedge corner suggests degrees of serpentinization as high as 50–60%. v_S, S-wave velocity.

serpentinized peridotite (Fig. 2c). Assuming a lower-crustal velocity of 3.6 km s^{-1}, the estimated maximum S-velocity perturbation of 10% near the wedge corner could represent a level of serpentinization as high as 50–60%. However, steadily diminishing levels are implied away from the corner as the velocity perturbation decreases through zero to normal polarity. Permeability within altered peridotite is likely to be fracture controlled, and the presence of free fluids may also serve to lower velocities. The degree of hydration diminishes eastwards, producing, in succession, reduced velocity contrast, disappearance of the aberrant Moho and, finally, restoration to a normal polarity crust–mantle boundary 40 km west of the arc.

In addition to a thermal model of Cascadia, we have produced thermal models for more typical cold continental (for example, northeast Japan) and oceanic (for example, Izu-Bonin) subduction zones. In cold subduction zones, the forearc temperatures are still lower, and in oceanic subduction zones with thin crust, the forearc mantle region is often larger. Thus although dimensions and geometry vary, all models predict the presence of a hydrated (and, hence, serpentinized) mantle wedge, suggesting that such structures are a generic feature of convergent margins. This inference is supported by recent studies in central Japan[17] and northern Chile[18] that employed travel times from local earthquakes to identify material with high Poisson's ratio above the subducting plate with serpentinized peridotite. Documentation of active serpentine mud volcanoes in the Mariana forearc[19] provides further supporting evidence.

The ubiquitous presence of a serpentinized mantle forearc in subduction zones has at least two important implications. It has been noted previously that the down-dip rupture limit of great subduction zone earthquakes in cold subduction zones usually coincides in depth with the continental Moho[20]. This observation can be explained through the presence of an altered mantle wedge[21]. Serpentine[22–24], and its companion alteration products brucite and talc[8], are believed to exhibit stable sliding behaviour at plate velocities, thus impeding rupture into the forearc mantle. A second consequence is that large-scale flow in the mantle wedge will be modified by the presence of serpentinized forearc mantle. In particular, the positive buoyancy and weak rheology of serpentine should serve to isolate most of the hydrated forearc wedge from the mantle-wedge corner flow system, while basal portions could be dragged down by the subducting plate. □

Received 21 December 2001; accepted 15 April 2002.

1. Gill, J. *Orogenic Andesites and Plate Tectonics* (Springer, New York, 1981).
2. Fyfe, W. S. & McBirney, A. R. Subduction and the structure of andesitic volcanic belts. *Am. J. Sci. A* **275,** 285–297 (1975).
3. Nabelek, J. L. *et al.* A high-resolution image of the Cascadia subduction zone from teleseismic converted phases recorded by a broadband seismic array. *Eos* **74,** 431 (1993).
4. Bostock, M. G., Rondenay, S. & Shragge, J. Multiparameter two-dimensional inversion of scattered teleseismic body waves 1. Theory for oblique incidence. *J. Geophys. Res.* **106,** 30771–30782 (2001).
5. Rondenay, S., Bostock, M. G. & Shragge, J. Multiparameter two-dimensional inversion of scattered teleseismic body waves 3. Application to the Cascadia 1993 data set. *J. Geophys. Res.* **106,** 30795–30807 (2001).
6. Peacock, S. M. Large-scale hydration of the lithosphere above subducting slabs. *Chem. Geol.* **108,** 49–59 (1993).
7. Fisher, A. T. Permeability within basaltic oceanic crust. *Rev. Geophys.* **36,** 143–182 (1998).
8. Peacock, S. M. & Hyndman, R. D. Hydrous minerals in the mantle wedge and the maximum depth of subduction thrust earthquakes. *Geophys. Res. Lett.* **26,** 2517–2520 (1999).
9. Ulmer, P. & Trommsdorff, V. Serpentine stability to mantle depths and subduction-related magmatism. *Science* **268,** 858–861 (1995).
10. Blackwell, D. D. *et al.* Heat flow in the Oregon Cascade Range and its correlation with regional gravity, Curie point depths, and geology. *J. Geophys. Res.* **95,** 19475–19493 (1990).
11. Lewis, T. J. *et al.* Subduction of the Juan de Fuca plate: thermal consequences. *J. Geophys. Res.* **93,** 15207–15227 (1988).
12. McMahon, A. *The Thermal Structure of the Cascadia Subduction Zone: Implications for Arc Magma Generation* Thesis, Arizona State Univ., Tempe (2001).
13. Christensen, N. Poisson's ratio and crustal seismology. *J. Geophys. Res.* **101,** 3139–3156 (1996).
14. Christensen, N. Elasticity of ultrabasic rocks. *J. Geophys. Res.* **71,** 5921–5931 (1966).
15. Ahrens, T. J. & Schubert, G. Gabbro-eclogite reaction rate and its geophysical significance. *Rev. Geophys. Space Phys.* **13,** 383–400 (1975).
16. Hacker, B. R. *et al.* in *Subduction Top to Bottom* (ed. Bebout, G. E.) 105–111 (American Geophysical Union, Washington DC, 1996).
17. Kamiya, S. & Kobayashi, Y. Seismological evidence for the existence of serpentinized wedge mantle. *Geophys. Res. Lett.* **27,** 819–822 (2000).
18. Graeber, F. M. & Asch, G. Three-dimensional models of P wave velocity and P-to-S velocity ratio in the southern central Andes by simultaneous inversion of local earthquake data. *J. Geophys. Res.* **104,** 20237–20256 (1999).
19. Fryer, P. Evolution of the Mariana convergent plate margin System. *Rev. Geophys.* **34,** 89–125 (1996).
20. Tichelaar, B. W. & Ruff, L. J. Depth of seismic coupling along subduction zones. *J. Geophys. Res.* **98,** 2017–2037 (1993).
21. Oleskevich, D. A., Hyndman, R. D. & Wang, K. The updip and downdip limits to great subduction earthquakes: thermal and structural models of Cascadia, south Alaska, SW Japan and Chile. *J. Geophys. Res.* **104,** 14965–14991 (1999).
22. Escartin, J., Hirth, G. & Evans, B. Strength of slightly serpentinized peridotites: Implications for the tectonics of oceanic lithosphere. *Geology* **29,** 1023–1026 (2001).
23. Raleigh, C. B. & Paterson, M. S. Experimental deformation of serpentinite and its tectonic consequences. *J. Geophys. Res.* **70,** 3965–3985 (1965).
24. Reinen, L. A. Seismic and aseismic slip indicators in serpentinite gouge. *Geology* **28,** 135–138 (2000).

Acknowledgements

We thank J. Nabelek and co-workers at Oregon State University for collecting the data set, and R. Benson for facilitating access to the IRIS DMC data archive.

Competing interests statement

The authors declare that they have no competing financial interests.

Correspondence and requests for materials should be addressed to M.G.B. (e-mail: bostock@geop.ubc.ca).

Common mammals drive the evolutionary increase of hypsodonty in the Neogene

Jukka Jernvall*† & Mikael Fortelius‡

** Developmental Biology Programme, Institute of Biotechnology, PO Box 56, FIN-00014, University of Helsinki, Helsinki, Finland*
† Department of Ecology and Systematics, PO Box 65; ‡ Department of Geology, PO Box 64, FIN-00014 University of Helsinki, Finland

During the past 20 million years, herbivorous mammals of numerous lineages have evolved hypsodont, or high-crowned, cheek teeth. Hypsodonty is informative ecologically because it is well developed in mammals eating fibrous and abrasive foods that are most abundant in open and generally or seasonally dry environments[1–5]. Here we report that in the Neogene of Europe mammals with the greatest locality coverages showed an increase in hypsodonty. We used a data set of 209 localities to measure whether large mammals occurring in many fossil localities show a similar increase in hypsodonty to mammals occurring in single or few localities. Taxonomic and morphological groupings show a low average hypsodonty in the early Miocene epoch. From the middle Miocene onwards, only the hypsodonty of commonly found mammals shows a marked increase. Therefore, in the drying Europe of the late Miocene, only increasingly hypsodont mammals may have been able to expand their share of habitats and food resources. These results suggest that the relatively small number of species known from multiple localities are palaeoecologically informative by themselves, irrespective of the rest of the known species.

Palaeoecological inference relies on information derived from individual fossil localities. Increased sampling and methods that correct for uneven sampling[6,7] or are insensitive to sampling[8,9] allow a more accurate, less biased description of evolutionary patterns. Large data sets including numerous localities now allow us to evaluate new aspects of community evolution, such as whether species found in many localities show similar palaeoecological